

Amyloid β -Protein Assembly and Alzheimer's Disease: Dodecamers of $A\beta_{42}$, but Not of $A\beta_{40}$, Seed Fibril Formation

Nicholas J. Economou,^{†,§} Maxwell J. Giammona,^{†,§} Thanh D. Do,[†] Xueyun Zheng,[†] David B. Teplow,[‡] Steven K. Buratto,^{*,†} and Michael T. Bowers^{*,†}

[†]Department of Chemistry and Biochemistry, University of California, Santa Barbara, California 93106, United States

[‡]Department of Neurology, David Geffen School of Medicine at UCLA; Mary S. Easton Center for Alzheimer's Disease Research at UCLA; and Brain Research Institute and Molecular Biology Institute, University of California, 635 Charles Young Drive South, Los Angeles, California 90095, United States

S Supporting Information

ABSTRACT: Evidence suggests that oligomers of the 42-residue form of the amyloid β -protein ($A\beta$), $A\beta_{42}$, play a critical role in the etiology of Alzheimer's disease (AD). Here we use high resolution atomic force microscopy to directly image populations of small oligomers of $A\beta_{42}$ that occur at the earliest stages of aggregation. We observe features that can be attributed to a monomer and to relatively small oligomers, including dimers, hexamers, and dodecamers. We discovered that $A\beta_{42}$ hexamers and dodecamers quickly become the dominant oligomers after peptide solubilization, even at low (1 μ M) concentrations and short (5 min) incubation times. Soon after (≥ 10 min), dodecamers are observed to seed the formation of extended, linear preprotofibrillar β -sheet structures. The preprotofibrils are a single $A\beta_{42}$ layer in height and can extend several hundred nanometers in length. To our knowledge this is the first report of structures of this type. In each instance the preprotofibril is associated off center with a single layer of a dodecamer. Protofibril formation continues at longer times, but is accompanied by the formation of large, globular aggregates. $A\beta_{40}$, by contrast, does not significantly form the hexamer or dodecamer but instead produces a mixture of smaller oligomers. These species lead to the formation of a branched chain-like network rather than discrete structures.

The amyloid β -protein ($A\beta$) is thought to play a seminal role in Alzheimer's disease (AD).¹ $A\beta$ is produced by serial endoproteolytic cleavage of the amyloid precursor protein, a type I transmembrane protein. These cleavages give rise to various forms of $A\beta$ that differ in length at their C-termini. The most abundant of these are 40 ($A\beta_{40}$) or 42 ($A\beta_{42}$) residues long (Scheme S1). Although the nominal concentration of $A\beta_{40}$ in humans is approximately 10 times that of $A\beta_{42}$, the latter peptide is most tightly linked to AD pathogenesis.² Early studies suggested that $A\beta$ fibril formation was the seminal neuropathogenic event in AD.³ For this reason, both $A\beta_{40}$ and $A\beta_{42}$ have been the subject of extensive studies of peptide aggregation.^{4–6} However, recent evidence has shown that soluble oligomeric forms of $A\beta$ now appear to be the most important effectors of the disease.^{1,7–9} If so, the development of oligomerization inhibitors would be facilitated by a more

rigorous understanding of the mechanisms by which initial $A\beta$ dimerization, and higher-order oligomer assembly, occur.¹⁰ The $A\beta$ monomer has been shown by NMR to fold into a strand-loop-strand conformation stabilized by intramolecular β -strand interactions. This folded conformation appears to facilitate the formation of the extended β -sheets that form mature amyloid fibrils.^{11–13} It has been suggested in AFM studies that small $A\beta$ oligomers act as seeds that induce oligomerization of adjacent monomers, similar to the mechanism of template-mediated prion conversion.^{6,14,15} Studies using ion-mobility based mass spectrometry (IMS-MS) have attempted to address exactly which types of oligomers are formed and whether these oligomers act as seeds for fibril growth.^{16,17} These studies revealed that even order oligomers were dominant, 2, 4, 6, and 12 with high populations of hexamers and dodecamers.¹⁷ The role played by these oligomers remains an open question, however. Understanding the amyloid initiation and growth mechanism in $A\beta$ would be very helpful in identifying therapeutic targets for effective AD disease treatment. We address this point later in this Communication

Atomic Force Microscopy (AFM) is an effective tool for visualizing large $A\beta$ structures such as fibrils^{6,14,15,18–21} and can also be used to gain information on the mechanical properties of these structures.^{22,23} Using AFM as a technique to image smaller structures such as monomers, dimers, and other small oligomers is highly desirable but carries with it significant challenges. The details of the AFM methods we use are given in the Supporting Information. AFM techniques by their nature have excellent vertical resolution, but their horizontal resolution is dependent on the geometry of the AFM tip. Folded $A\beta$ monomers are extremely small (~ 2 nm in diameter),^{24,25} which makes them difficult to resolve unless extremely sharp AFM tips are used. The Smith group at SUNY Stony Brook used super sharp tips to collect images of $A\beta_{42}$ at early stages of aggregation.^{6,26,27} They were able to distinguish various oligomers and to propose a model for how their growth occurs.²⁶ They theorize that β -sheet-like dimers can directly associate to form protofibrils which then go on to form fibrils. They also suggest oligomers with β -sheet content can be formed in a parallel pathway and these oligomers eventually

Received: November 13, 2015

Published: February 2, 2016

rearrange to form fibrils. However, certain aspects of the conclusions of this study do not agree well with other models for oligomer aggregation.^{16,17,28} Here, we seek to obtain a more complete picture of the time dependence of the oligomer population in solution by altering the sample preparation technique.

Figure 1 shows representative AFM topography images of A β 42 using super sharp tips at solution incubation times of 5

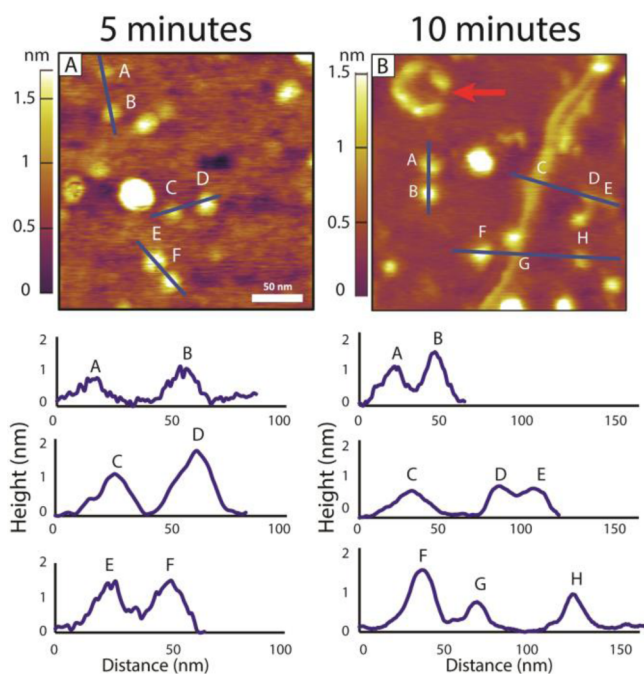


Figure 1. Representative AFM topography images of A β 42 after (A) 5 and (B) 10 min of incubation in a 1 μ M solution. Below each image are line cuts illustrating the heights of the observed features. (A) Features A, B, and C indicate A β hexamers, and D, E, and F indicate A β dodecamers consisting of two stacked hexamers. (B) shows that hexamers and dodecamers are still present after 10 min. Features C and G show a preprotofibril structure.

and 10 min. In all images shown here, the sample has been directly deposited on the mica surface without further treatment. We found rinsing the surface following deposition resulted in removal of a large fraction of deposited material making it impossible to follow structural evolution as incubation time increased. See SI for details. At 5 min, we see almost exclusively small circular aggregates with heights principally between 0.75 and 1.50 nm. We attribute these features to single (0.75 nm) or double (1.5 nm) layers of A β 42. Most of these features have a circular profile consistent with previous AFM studies.^{6,26,27} The observed diameters are 10 to 15 nm measured by the base width. Previous IMS-MS data show the dominant oligomers in solution under conditions similar to those used here are hexamers and dodecamers.^{16,17} The cross sections reported for the hexamer and dodecamer structures agree well with the dimensions of the features in Figure 1A after tip deconvolution.^{16,17} Hence, given the circular profile and the measured dimensions we assign the features in Figure 1 with heights under 1 nm as hexamers and those near 1.5 nm as dodecamers. We also see a very low density of structures at 2.25 and 3 nm heights. These are not predicted to be abundant based on mass spectrometry studies.^{16,17} It is possible that these larger features correspond to amorphous

aggregates of several smaller oligomers, as they often have a larger diameter (\sim 25 nm) than the hexamer or dodecamer.

In the bottom half of Figure 1A are plotted line cuts through selected features in the image above giving the heights along the line. Features A, B, and C have heights less than 1 nm associated with single layer oligomers. We assign these features to hexamers. Features D, E, and F are approximately twice as high as A, B, and C, and hence we assign these features as dodecamers. There are no elongated, fibril-like features present at the 5 min incubation time.

Figure 1B is an image taken at a 10 min incubation time. Many of the 5 min features are still present, but new features are also evident. For example, in the upper left of Figure 1B is what appears to be 6 circular objects interacting with each other to form a quasi-circular construct (see arrow in Figure 1B). Height and width measurements indicate each of the 6 individual features are hexamers (data not shown). Such a feature is rare and does not increase in frequency with incubation time but does indicate there is a tendency for hexamers to interact with each other in this manner. Even more interesting is the appearance of a long, narrow filament-like structure in the right half of the image (over 200 nm long). Line cut height data (given below the image) indicate features B and F are dodecamers while A, D, E, and H are hexamers. The filament is 0.7 nm high (features C and G) and has an average width of approximately 10 nm. Given its physical characteristics we term this feature as a “pre-*protofibril*” and discuss it in more detail shortly.

Longer time images are given in Figure 2. By 20 min the density of preprotofibrils has grown considerably. The line cut E verifies these abundant species have heights of only 0.7 nm and widths of approximately 10 nm. Their lengths are clearly greater than 250 nm, as they extend beyond the image area in both directions. The larger spherical aggregates have also grown in frequency while the dodecamers and hexamers, although diminished in relative frequency, are still present (line cut A,B). These trends continue as evidenced by the 60 min image given in Figure 2B. Here clumping of the large spherical aggregates is clearly observed, consistent with earlier AFM studies taken at higher concentrations and longer incubation times.^{26,27}

In summary we emphasize the *solution* evolution of the features observed in Figures 2 and 3. In all cases the solution spent approximately 2 min being vacuum-dried after being drop cast on the mica. As a consequence, the different structures observed are directly related to the incubation time in solution and not to surface–A β interactions. This point is more fully discussed in the Supporting Information.

A portion of the 10 min image is expanded and given as Figure 3A. There are two circular features shown as well as a portion of the preprotofibril. The left-most feature is feature F in Figure 1B and has been assigned as a dodecamer. The second circular feature is also a dodecamer, as determined by height and width measurements (data not shown). The most interesting and important aspect of this image is the fact the long preprotofibril appears to be growing out of the lower hexamer of the dodecamer. There has long been a view that A β fibrils were seeded by smaller structures, but until now there has been no direct evidence of the nature of the seed. There are essentially two limiting mechanisms that have been put forward for fibril growth in A β solutions.^{1,27,29} The first one involves initial formation of a “seed” oligomer followed by monomer templating and addition to form β -sheet structured prefibrils that eventually become fibrils (the nucleated polymerization

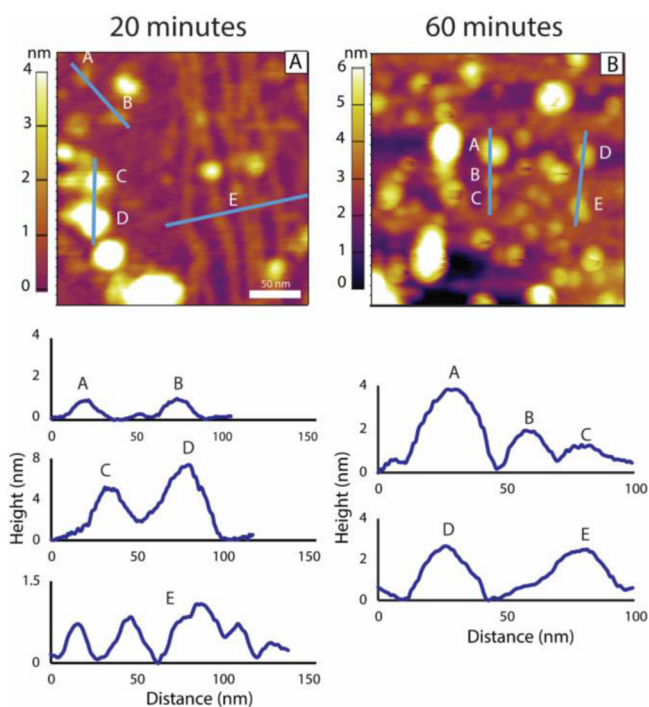


Figure 2. Representative AFM topography images of $A\beta_{42}$ after (A) 20 and (B) 60 min of incubation in a $1 \mu\text{M}$ solution. Below each image are line cuts illustrating the heights of the observed features. (A) shows that after 20 min while dodecamers sized structures are still present (features A and B) a much higher density of larger globular aggregates has also formed (features C and D). Also present is a much larger amount of the preprotofibril structures shown by feature E. (B) shows that, after 60 min, large globular aggregates have come to dominate the morphology.

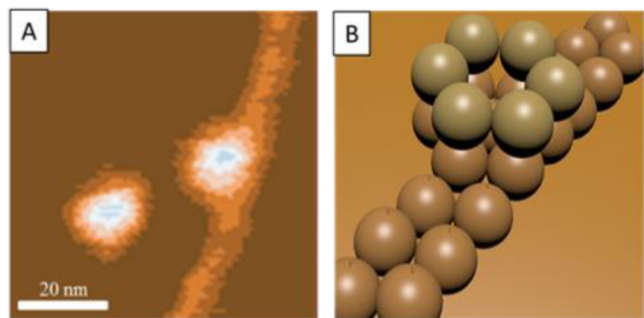


Figure 3. (A) Topographic image of $A\beta_{42}$ cast from a $1 \mu\text{M}$ solution after 10 min of incubation showing the interaction between dodecamers and extended preprotofibrils. (B) Schematic cartoon of this growth mechanism.

mechanism).³⁰ The second involves $A\beta$ oligomer condensation to form protofibrils directly (the nucleated conformational conversion pathway).³¹ In this latter pathway it is ambiguous how and when β -sheet based structures are formed.

In a time sequence, dodecamers appear early on and then later in time filaments appear and are always associated with dodecamers (Figures 1 and 3). Hence the data strongly implicate the dodecamers as the seeds for the earliest fibril formation. These preprotofibrils have all of the physical characteristics of the β -sheet structures found experimentally in $A\beta_{42}$ fibrils.³² This is, to our knowledge, the first direct observation of the connection between known $A\beta_{42}$ assemblies (hexamers and dodecamers) and the fibrils themselves.^{16,17}

This observation unambiguously shows the dodecamer as “on pathway” for fibril formation, an unanswered question up to this point. There has previously been evidence that the dodecamer is a likely proximate toxic agent in transgenic mice studies.³³ Hence there must be a delicate interplay between the dodecamer acting as the toxic agent in AD and its tendency to seed fibril formation. The latter process produces insoluble aggregates that are less toxic than the oligomers and may actually be protective.³⁴ The $A\beta_{42}$ dodecamer is emerging as the central player in the molecular basis for Alzheimer’s disease.

The dominant alloform of the $A\beta$ -protein in vivo is $A\beta_{40}$, typically making up 90% of the $A\beta$ -protein present.² Previous studies have indicated that $A\beta_{40}$ forms fibrils more slowly than $A\beta_{42}$ and by a different mechanism.^{35,36} IMS-MS experiments unambiguously showed $A\beta_{40}$ forms tetramers as the terminal oligomer species while $A\beta_{42}$ formed dodecamers as the terminal oligomer species.^{16,17} Our AFM results for $A\beta_{40}$ are summarized in Figure 4.

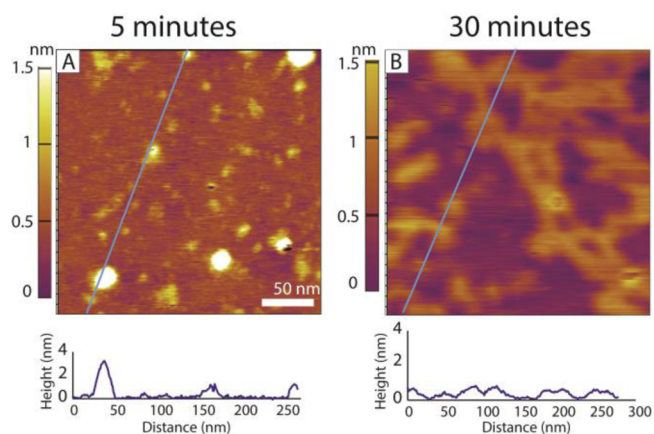


Figure 4. Representative AFM topography images of $A\beta_{40}$ incubated after (A) 5 and (B) 30 min of incubation in a $1 \mu\text{M}$ solution. Below each image is a line cut to illustrate the height of the features present. In (A) the morphology is dominated by much smaller features than were observed at this time for $A\beta_{42}$. (B) shows a peptide film of constant height that deposited onto the surface suggesting that most of the protein remains in the monomer or other low order oligomer state, weakly associated in solution.

Figure 4A shows a low density of spherical features. The mica surface is coated with monomers and very small oligomers (dimers and tetramers) with the occasional larger spherical aggregate as shown by the line cut below the image. At longer incubation times the few spherical aggregates diminish in frequency as shown in the 30 min image in Figure 4B. This image is dominated by a highly branched network of chain-like segments 1 nm or less in height and 10 nm in width on average, suggesting the network is β -sheet in character.³² This network continues to develop at longer times until monomer and small oligomers are no longer available (data not shown). At no time frame (5 to 60 min) do we observe long single preprotofibrils in any of the $A\beta_{40}$ images, nor do we observe the onset of any portion of this branched network with a specific oligomer as was observed for $A\beta_{42}$ (Figure 3). These results are fully consistent with earlier ion mobility studies where oligomer formation in $A\beta_{40}$ terminated at the tetramer.¹⁶ They also correlate with the fact that $A\beta_{40}$ is much less toxic than $A\beta_{42}$ and that oligomers of $A\beta_{40}$ were not observed in transgenic

mice studies while those of A β 42 were observed.^{33,34} In addition it has been observed that hetero-oligomers of A β 40 and A β 42 terminate at the tetramer which suggests that A β 40 is cyto-protective rather than cyto-toxic.³⁷

In summary, we have used high resolution atomic force microscopy to probe the earliest stages of A β aggregation. We have shown direct evidence that A β 42 undergoes rapid formation of hexamers and dodecamers with the dodecamers seeding the formation of extended preprotofibrils. Larger globular structures form at longer incubation times. A β 40, on the other hand, undergoes a different assembly mechanism where hexamers and dodecamers are not involved resulting in the formation of what appear to be branched β -sheet structures and a much lower frequency of large globular aggregates. These results are fully consistent with earlier data from IMS-MS and other methods and give molecular insight into why A β 42 is the central player in the molecular basis of Alzheimer's disease and why A β 40 is not.

■ ASSOCIATED CONTENT

● Supporting Information

The Supporting Information is available free of charge on the ACS Publications website at DOI: 10.1021/jacs.5b11913.

Included are the AFM methodology used, sample preparation techniques, images comparing the rinse and no rinse sample preparations methods, larger scale (5 μ M) images of A β 42 at each incubation time and A β 40 after 30 min (PDF)

■ AUTHOR INFORMATION

Corresponding Authors

*buratto@chem.ucsb.edu

*bowers@chem.ucsb.edu

Author Contributions

§N.J.E. and M.J.G. contributed equally.

Notes

The authors declare no competing financial interest.

■ ACKNOWLEDGMENTS

We are grateful to acknowledge the support of the National Institute of Health Grant Number 1R01AG047116-01 (M.T.B.).

■ REFERENCES

- Roychaudhuri, R.; Yang, M.; Hoshi, M. M.; Teplow, D. B. *J. Biol. Chem.* **2009**, *284*, 4749.
- Younkin, S. G. *Ann. Neurol.* **1995**, *37*, 287.
- Hardy, J.; Higgins, G. *Science* **1992**, *256*, 184.
- Snyder, S.; Lador, U.; Wade, W.; Wang, G.; Barrett, L.; Matayoshi, E.; Huffaker, H.; Krafft, G.; Holzman, T. *Biophys. J.* **1994**, *67*, 1216.
- Goldsbury, C. S.; Wirtz, S.; Müller, S. A.; Sunderji, S.; Wicki, P.; Aebi, U.; Frey, P. *J. Struct. Biol.* **2000**, *130*, 217.
- Ahmed, M.; Davis, J.; Aucoin, D.; Sato, T.; Ahuja, S.; Aimoto, S.; Elliott, J. L.; Van Nostrand, W. E.; Smith, S. O. *Nat. Struct. Mol. Biol.* **2010**, *17*, 561.
- Harper, J. D.; Wong, S. S.; Lieber, C. M.; Lansbury, P. T., Jr. *Chem. Biol.* **1997**, *4*, 119.
- Bernhardt, N. A.; Berhanu, W. M.; Hansmann, U. H. E. *J. Phys. Chem. B* **2013**, *117*, 16076.
- Demuro, A.; Mina, E.; Kaye, R.; Milton, S. C.; Parker, I.; Glabe, C. G. *J. Biol. Chem.* **2005**, *280*, 17294.
- Teplow, D. B. *Alzheimer's Res. Ther.* **2013**, *5*, 39.
- Hou, L. M.; Shao, H. Y.; Zhang, Y. B.; Li, H.; Menon, N. K.; Neuhaus, E. B.; Brewer, J. M.; Byeon, I. J. L.; Ray, D. G.; Vitek, M. P.; Iwashita, T.; Makula, R. A.; Przybyla, A. B.; Zagorski, M. G. *J. Am. Chem. Soc.* **2004**, *126*, 1992.
- Sticht, H.; Bayer, P.; Willbold, D.; Dames, S.; Hilbich, C.; Beyreuther, K.; Frank, R. W.; Rosch, P. *Eur. J. Biochem.* **1995**, *233*, 293.
- Vivekanandan, S.; Brender, J. R.; Lee, S. Y.; Ramamoorthy, A. *Biochem. Biophys. Res. Commun.* **2011**, *411*, 312.
- Harper, J. D.; Lieber, C. M.; Lansbury, P. T., Jr. *Chem. Biol.* **1997**, *4*, 951.
- Serem, W. K.; Bett, C. K.; Ngunjiri, J. N.; Garno, J. C. *Microsc. Res. Tech.* **2011**, *74*, 699.
- Bernstein, S. L.; Dupuis, N. F.; Lazo, N. D.; Wyttenbach, T.; Condrón, M. M.; Bitan, G.; Teplow, D. B.; Shea, J.-E.; Ruotolo, B. T.; Robinson, C. V.; Bowers, M. T. *Nat. Chem.* **2009**, *1*, 326.
- Bernstein, S. L.; Wyttenbach, T.; Baumketner, A.; Shea, J.-E.; Bitan, G.; Teplow, D. B. *J. Am. Chem. Soc.* **2005**, *127*, 2075.
- Parbhu, A.; Lin, H.; Thimm, J.; Lal, R. *Peptides* **2002**, *23*, 1265.
- Qiang, W.; Kelley, K.; Tycko, R. *J. Am. Chem. Soc.* **2013**, *135*, 6860.
- Zhou, X.; Zhang, Y.; Zhang, F.; Pillai, S.; Liu, J.; Li, R.; Dai, B.; Li, B.; Zhang, Y. *Nanoscale* **2013**, *5*, 4816.
- Stine, W. B.; Snyder, S. W.; Lador, U. S.; Wade, W. S.; Miller, M. F.; Perun, T. J.; Holzman, T. F.; Krafft, G. A. *J. Protein Chem.* **1996**, *15*, 193.
- Raman, E. P.; Takeda, T.; Barsegov, V.; Klimov, D. K. *J. Mol. Biol.* **2007**, *373*, 785.
- Hane, F. T.; Lee, B. Y.; Petoyan, A.; Rauk, A.; Leonenko, Z. *Biosens. Bioelectron.* **2014**, *54*, 492.
- Losic, D.; Martin, L. L.; Mechler, A.; Aguilar, M. I.; Small, D. H. *J. Struct. Biol.* **2006**, *155*, 104.
- Baumketner, A.; Bernstein, S. L.; Wyttenbach, T.; Bitan, G.; Teplow, D. B.; Bowers, M. T.; Shea, J.-E. *Protein Sci.* **2006**, *15*, 420.
- Mastrangelo, I. A.; Ahmed, M.; Sato, T.; Liu, W.; Wang, C.; Hough, P.; Smith, S. O. *J. Mol. Biol.* **2006**, *358*, 106.
- Fu, Z.; Aucoin, D.; Davis, J.; Van Nostrand, W. E.; Smith, S. O. *Biochemistry* **2015**, *54*, 4197.
- Bleiholder, C.; Dupuis, N. F.; Wyttenbach, T.; Bowers, M. T. *Nat. Chem.* **2011**, *3*, 172.
- Cohen, S. I. A.; Linse, S.; Luheshi, L. M.; Hellstrand, E.; White, D. A.; Rajah, L.; Otzen, D. E.; Vendruscolo, M.; Dobson, C. M.; Knowles, T. P. J. *Proc. Natl. Acad. Sci. U. S. A.* **2013**, *110*, 9758.
- Harper, J. D.; Lansbury, P. T. *Annu. Rev. Biochem.* **1997**, *66*, 385.
- Serio, T. R.; Cashikar, A. G.; Kowal, A. S.; Sawicki, G. J.; Moslehi, J. J.; Serpell, L.; Arnsdorf, M. F.; Lindquist, S. L. *Science* **2000**, *289*, 1317.
- Walsh, D. M.; Lomakin, A.; Benedek, G. B.; Condrón, M. M.; Teplow, D. B. *J. Biol. Chem.* **1997**, *272*, 22364.
- Lesné, S.; Koh, M. T.; Kotilinek, L.; Kaye, R.; Glabe, C. G.; Yang, A.; Gallagher, M.; Ashe, K. H. *Nature* **2006**, *440*, 352.
- Cheng, I. H.; Scarce-Levie, K.; Legleiter, J.; Palop, J. J.; Gerstein, H.; Bien-Ly, N.; Puoliväli, J.; Lesné, S.; Ashe, K. H.; Muchowski, P. J.; Mucke, L. *J. Biol. Chem.* **2007**, *282*, 23818.
- Bitan, G.; Kirkitadze, M. D.; Lomakin, A.; Vollers, S. S.; Benedek, G. B.; Teplow, D. B. *Proc. Natl. Acad. Sci. U. S. A.* **2003**, *100*, 330.
- Roychaudhuri, R.; Yang, M.; Deshpande, A.; Cole, G. M.; Frautschy, S.; Lomakin, A.; Benedek, G. B.; Teplow, D. B. *J. Mol. Biol.* **2013**, *425*, 292.
- Murray, M. M.; Bernstein, S. L.; Nyugen, V.; Condrón, M. M.; Teplow, D. B.; Bowers, M. T. *J. Am. Chem. Soc.* **2009**, *131*, 6316.